



**HAL**  
open science

# Hot-electron three-terminal devices based on magnetic tunnel junction stacks

Michel Hehn, François Montaigne, Alain Schuhl

► **To cite this version:**

Michel Hehn, François Montaigne, Alain Schuhl. Hot-electron three-terminal devices based on magnetic tunnel junction stacks. *Physical Review B*, 2002, 66 (14), pp.144411. 10.1103/PhysRevB.66.144411 . hal-04370131

**HAL Id: hal-04370131**

**<https://hal.science/hal-04370131v1>**

Submitted on 1 Aug 2024

**HAL** is a multi-disciplinary open access archive for the deposit and dissemination of scientific research documents, whether they are published or not. The documents may come from teaching and research institutions in France or abroad, or from public or private research centers.

L'archive ouverte pluridisciplinaire **HAL**, est destinée au dépôt et à la diffusion de documents scientifiques de niveau recherche, publiés ou non, émanant des établissements d'enseignement et de recherche français ou étrangers, des laboratoires publics ou privés.

**Hot-electron three-terminal devices based on magnetic tunnel junction stacks**

M. Hehn, F. Montaigne, and A. Schuhl

*Laboratoire de Physique des Matériaux, UMR CNRS 7556, BP 239, 54506 Vandoeuvre lès Nancy Cedex, France*

(Received 22 October 2001; revised manuscript received 14 January 2002; published 21 October 2002)

Magnetic-configuration-dependent electrical characteristics of magnetic-tunnel-junction-based three-terminal devices have been computed in the framework of the parabolic band model. Besides their fundamental interest in measuring the properties of nonequilibrium spin-dependent hot-electron transport, three-terminal devices appear to be good candidates for a new generation of magnetic-field-dependent devices. The control of the hot-electron transmission in a double-tunnel junction is a keystone to ensure asymmetric diodes or hot-electron magnetic-field-dependent transistors. Based on a basic description of electron scattering and noncoherent transport in the structure but using electronic parameters extracted from experiments, we assess the functionalities of those devices.

DOI: 10.1103/PhysRevB.66.144411

PACS number(s): 73.40.Gk, 73.40.Rw, 72.25.Mk

**I. INTRODUCTION**

The discovery of a tunnel magnetoresistance (TMR) effect at room temperature in oxide-barrier-based magnetic tunnel junctions<sup>1</sup> (MTJ's) paved the way to intense developments of this field area with many possible application prospects.<sup>2</sup> Those numerous studies devoted to different aspects of this topic permit getting a better understanding of the fundamentals of spin-polarized tunneling transport. From the experimental point of view, a large effort was paid to optimize the growth of thin insulating materials<sup>3</sup> and to study magnetization reversal processes, domain formation, and their implications to the TMR signal.<sup>4,5</sup> From the theoretical point of view, the magnetotransport properties were modeled using a transfer Hamiltonian,<sup>6</sup> free-electron-like models,<sup>7</sup> or more sophisticated band structure calculations.<sup>8</sup> Much of the attention was then paid to the study of single-tunnel-barrier structures and the quality of the grown materials allows us now to pass a further step.

Indeed, as was previously remarked by Mead<sup>9</sup> in the early 1960s, *a new class of devices employing the principle of electron tunnel emission from a metal-insulator-metal diode where the second metal layer is thin can be built. A triode geometry can then be secured by the addition of a second insulator and a metal collector layer.* The proposed structure is not less than a double-tunnel-barrier junction. Up to now, few studies have been devoted to the development of such structures.<sup>10</sup> A transistor effect has been shown in the particular case of an epitaxial  $M/I/M/I/M$  structure where  $I$  is  $\text{CaF}_2$  and  $M$  is  $\text{CoSi}_2$  (Ref. 11) (analog effects are observed in similar semiconductor structures<sup>12</sup>). However, the need of epitaxy and the lack of magnetism limit the couple of  $M/I$  which can be used and no spin-dependent transport can occur. Recently, new experimental achievements have emerged with the development of the hot-electron spin-valve transistor<sup>13</sup> or the magnetotunneling injection device.<sup>14</sup> In both systems, spin-dependent tunneling governs the electron transport in the structure. Nevertheless, in the former, hot electrons are concerned but there is a need for a crystalline Si emitter and collector and, in the latter, spin accumulation seems to be at the origin of the magnetoresistance.

In this paper, we propose to combine spin-polarized hot-

electron transport with a magnetic-tunnel-junction-based three-terminal device. This way, we fully relax the constraints related to the epitaxy of  $M/I$  or Si layers and so enlarge the number of material combinations to make the desired  $M_1/I_1/M_2/I_2/M_3$  structure. The complete stack can then be made with a sputtering machine; the layers can be amorphous, but we show from a theoretical basis that a hot-electron transfer can be obtained from  $M_1$  to  $M_3$  as was shown in Ref. 13. Based on experimental tunnel barrier parameters, magnetic-field-dependent electrical characteristics of magnetic-tunnel-junction-based three-terminal devices have been computed in the framework of the parabolic band model. They assess the functionalities of a new generation of magnetic-field-dependent devices like asymmetric diodes or hot-electron magnetic-field-dependent transistors based on the control of the hot-electron transmission. Furthermore, besides their applied interest,  $M_1/I/M_2/I/M_3$  structure can be used to measure the properties of nonequilibrium spin-dependent hot-electron transport. Indeed, thanks to an energy injection in the range of 0.5–4 eV (depending on the voltage breakdown of  $I_1$ ), these studies will complete those dedicated to hot electrons injected from vacuum<sup>15,16</sup> with energies above 3 eV.

After a description of the theoretical model developed to calculate the spin-dependent transport in  $M_1/I/M_2/I/M_3$  structures with an electrical contact on each  $M_i$  layer, we give some examples of its use for magnetically programmable devices.

**II. THEORETICAL DETAILS**

In this section, we give the main aspects of the theoretical model which has been used to calculate the field-dependent transport characteristics of hot-electron three-terminal devices based on magnetic tunnel junction stacks (3TD-MTJ). The potential profile of the 3TD-MTJ system under consideration is shown in Fig. 1, where  $\phi_i$  and  $d_i$  are, respectively, the barrier height and thickness of the barrier number ( $i$ ). The barriers are considered as rectangular in the absence of any applied voltage. Due to the high conductivity of the metallic electrodes, the voltage drop is distributed homogeneously only in the barriers leading to the barriers skewing

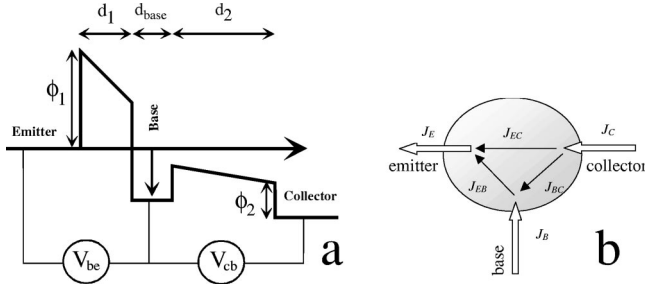


FIG. 1. (a) Potential profile of the hot-electron three-terminal device based on magnetic tunnel junction stacks under applied voltage. (b) Definition of the current densities flowing through the three-terminal device.

under given bias voltage. The voltage applied to those tunnel barriers is referenced as  $V_{BE}$  and  $V_{CB}$ . The spin-polarized current pumped from the emitter-base (EB) junction biased with voltage  $V_{BE}$  is injected in the base magnetic electrode with an energy  $e \times V_{BE}$  above the Fermi level of the base electrode. If the thickness of the base is large compared to the mean free path of the electrons,  $\lambda$ , each electron extracted from the emitter electrode would be thermalized in the base and each junction would behave independently just like two resistors in series. If the thickness of the base is comparable to  $\lambda$ , some electrons injected from the emitter to the base can travel through the base without being scattered (ballistic transport) and eventually pass the base-collector (BC) barrier. As the tunneling probability increases exponentially with the energy, the transmission of the hot electrons is much higher than the one coming from the base Fermi level and can be controlled with the  $V_{CB}$  voltage, leading to the appearance of an asymmetric current-voltage characteristic.

Modeling of this device requires calculation of several tunnel currents: the total injected current  $J_E$  going through the EB barrier depends only on the parameters of this barrier (and particularly the applied voltage  $V_{BE}$ ) independently of the processes of energy relaxation in the base or if the electrons will pass or not the BC barrier. Similarly the current of thermal electrons from the base to the collector  $J_{BC}$  (or from the collector to the base if  $V_{CB}$  is negative) only depends on the BC barrier. We consider here that the electrons thermalized in the base have relaxed both their energy and their spin. The ballistic current  $J_{EC}$  is more complex. It depends on the electron probability to pass the EB barrier, the energy relaxation processes in the base and the probability to pass the BC barrier. Multiple reflections in the base must also be considered since an electron can be reflected by the BC and then the EB barrier. Other currents are simply deduced from node laws.

The transport of hot electrons injected in the base results from several complex phenomena and the situation is even more complex in a ferromagnetic metal in which this transport is spin dependent. Different scattering events, elastic or inelastic, are possible including scattering by phonons, magnons, Stoner excitations (Ref. 17 gives a theoretical study of these two last phenomenon), defects, and interfaces. In the energy range of interest here, these transport phenomena can be studied by ballistic electron emission microscopy<sup>18</sup>

(BEEM) or thanks to the spin-valve transistor.<sup>13</sup> From these experiments, an attenuation factor is measured and its exponential thickness dependence allows us to define an attenuation length  $\lambda$ . This length is an effective value including all the processes decreasing the transmission. Inelastic scattering is obviously a major contribution to  $\lambda$  since any loss of energy for an electron will decrease exponentially its probability of being transmitted through the BC barrier. But elastic scattering also contributes to the attenuation. As a matter of fact, the conduction through tunnel barriers being exponentially dependent on the perpendicular to multilayer planes wave vector  $k_z$ , the electrons injected in the base move essentially perpendicularly to the plane of the layers (this effect is increased by the electric field present in the emitter-base barrier which accelerates the electrons in the perpendicular direction). The probability for an electron in the base to be transmitted through the base-collector barrier is also exponentially dependent on  $k_z$ . Any elastic scattering in the base will statistically deviate the electron from its direction perpendicular to the film plane and thus decrease its probability of being transmitted in the collector. Inelastic and elastic scatterings have thus the same effect, i.e., a reduction of the “direct” emitter to collector current.<sup>19</sup> Any scattered electron thus decreases exponentially its probability of transmission and will increase its path in the base by reflection on the barriers. In turn, its probability of being further scattered increases and this until complete thermalization occurs. We will thus consider in our model that any scattering event, elastic or inelastic, decreases the transmission probability to negligible values and leads to the thermalization of the electron. This approach is different from the one adopted by Zhang<sup>20</sup> who has considered in a similar structure, a progressive relaxation of the electron energy. In this vision, every electron impinges on the BC barrier with the same energy which is its initial energy multiplied by a constant term, exponentially decreasing with the thickness of the base. Thus, there is no electron conserving its initial energy and there is no momentum conservation. However, our approach is supported by earlier calculations from Ref. 21 considering inelastic scattering which show that the number of ballistic electrons conserving their initial energy decreases exponentially whereas a tail of low energy above the base Fermi level appears.

Furthermore, coherent transport through the base has not been considered for simplicity and also to show that even without coherence, highly probable in our 3TD-MTJ, hot-electron-related phenomena can be expected.

With this approximation, the probability for a hot electron from the emitter to be injected in the base, and pass the base and BC barrier is

$$D_{EB}(V_{BE})\exp(-d/\lambda)D'_{BC}(V_{CB}), \quad (1)$$

where  $d$  is the effective thickness of the base.  $D_{EB}$  and  $D'_{BC}$  are, respectively, the transmission probability through the EB and BC barriers (the prime indicates that the transmission probability of hot electrons has to be considered). They are separately deduced from the wave functions in barrier and the electrodes, solutions of the Schrödinger equation.

Similarly, the probability for being reflected by the BC barrier is

$$D_{EB}(V_{BE})\exp(-d/\lambda)[1 - D'_{BC}(V_{CB})]. \quad (2)$$

The probability for being transmitted after this reflection on the BC and then the EC barrier is thus

$$D_{EB}(V_{BE})\exp(-d/\lambda)[1 - D'_{BC}(V_{CB})] \\ \times \exp(-2d/\lambda)D'_{BC}(V_{CB}). \quad (3)$$

By extending this to an infinite number of reflections, one can obtain the ‘‘hot’’ transmission probability

$$D_{EC} = D_{EB}(V_{BE})D'_{BC}(V_{CB}) \\ \times \frac{\exp(-d/\lambda)}{1 - \exp(-2d/\lambda)[1 - D'_{BC}(V_{CB})]}. \quad (4)$$

Finally following Tsu and Esaki<sup>22</sup> and considering motion parallel and perpendicularly to the barrier, at low temperature, the different transmission probabilities have simply to be integrated over an adequate range of energy

$$J_E = \frac{2\pi e}{h^3} m_e^* \int \int D_{EB}(E_z, E_{\parallel}) dE_z dE_{\parallel}, \quad (5)$$

$$J_{EC} = \frac{2\pi e}{h^3} m_e^* \int \int D_{EC}(E_z, E_{\parallel}) dE_z dE_{\parallel}, \quad (6)$$

$$J_{BC} = \frac{2\pi e}{h^3} m_b^* \int \int D_{BC}(E_z, E_{\parallel}) dE_z dE_{\parallel}, \quad (7)$$

where  $E_z$  ( $E_{\parallel}$ ) is the electron energy perpendicular (parallel) to the tunnel barriers in the emitter electrode, and  $m_e^*$  and  $m_b^*$  are the effective electron masses in the emitter and base electrode, respectively.

A rigorous free electron model has been used in order to compute those currents and therefore we have taken into account the transverse (in-plane) motion of the electrons. Indeed, refraction of the electron at the barrier interface, due to the difference of effective mass between the metal and insulator, allows tunneling of additional electrons. Therefore,  $D$  cannot be simply integrated over  $E_z$  but a two-dimensional integration over  $E_{\parallel}$  and  $E_z$  has to be done. This double integration has been shown in a previous work<sup>7</sup> to be of primary importance. As we focus here on the transport of hot electrons and in order to simplify the computations, the simplest band structure for the different materials, i.e., parabolic bands (free electron), has been used. This does not allow us to address directly the effects of interface magnons or phonons<sup>23</sup> or the effects of complex band structure on the TMR.<sup>24</sup> Nevertheless, we have shown that this model can predict qualitatively the complex  $MR(V)$  observed in composite barriers.<sup>7</sup> Therefore we are confident in the results shown in this paper even if additional features can appear with sophisticated materials.

To model those bands, we used the parameters proposed by Davis and MacLaren<sup>25</sup> for iron. For the spin-up (-down) band, we have a Fermi level at 2.25 eV (0.5 eV) and an effective mass equal to 1.27 (1.36) times the free electron mass. However, as was stressed in a previous paper,<sup>7</sup> a change of the band parameters does not change drastically the results reported in this paper. The barrier parameters have been chosen to fit the current-voltage characteristics of real tunnel junctions. Therefore,  $\phi$  values of 1.5 and 0.5 eV have been used because they have been shown to be reached using aluminum oxide<sup>4</sup> and tantalum oxide<sup>26</sup> tunnel barriers, respectively. As was recently shown by Stein *et al.*,<sup>14</sup> it is experimentally proved that an electric contact can be taken on a 5-nm-thick base layer made with ferromagnetic materials. We have thus chosen this value for our computations. A mean free path of 5 nm (2.5 nm) for the spin-up (-down) electrons has been chosen in accordance with the recent measurements made by Vlutters *et al.*<sup>27</sup> Finally, the electron mass in the barrier was taken equal to  $0.4m_e$ , the estimated value computed for crystalline alumina and in the range of values measured for amorphous  $\text{SiO}_2$ . This set of parameters has been used to fit experimental conditions that can be reached in the near future in order to bring soon an experimental verification of those calculations. The electrical characteristics of the 3TD-MTJ have been computed considering two independent spin channels and colinear alignment of the electrode magnetizations with two magnetization configurations: (i) the parallel magnetizations of the three  $M_i$  layers and (ii) the magnetization of  $M_2$  antiparallel to the magnetizations of  $M_1$  and  $M_3$ . The TMR of a given current (emitter, base, or collector current) is then calculated from the difference of the currents calculated in the parallel and antiparallel magnetization states divided by the current calculated in the antiparallel magnetization state. Those configurations are readily obtained experimentally when parallel easy magnetic axes are defined in each  $M_i$  layer and when  $M_2$  has the lowest coercive field. The reversal of  $M_2$  can then be achieved for example with the field created by a current going through the connection lead of  $M_1$  and/or  $M_3$  as is in the new generation of magnetic tunnel memories.<sup>28</sup> Furthermore, more complex magnetic configurations like an angle between  $M_2$  and  $M_1, M_3$  can be accessed using an additional electric line that can create a field perpendicular to the  $M_2$  easy axis but are not treated in those calculations.

This rigorous free electron model and those parameters were applied to compute the magnetic-configuration-dependent electrical characteristics of 3TD-MTJ-based devices.

### III. THREE-TERMINAL CURRENT-VOLTAGE ASYMMETRIC DEVICES

The use of magnetic tunnel junctions is predicted for the next generation of nonvolatile magnetic random access memories (MRAM). Indeed, they combine high-speed, low-power consumption and dissipation, nonvolatility, high packing density, and low cost. However, a silicon diode or a transistor is needed in series with each MTJ cell to avoid leakage current in the MRAM cell array during the reading

operation. This diode limits the current state-of-the-art packing density. Alternatives to the use of this diode are currently under development and two of those are presented in the following. It appears that the association of a silicon device and a MTJ can be replaced by one 3TD-MTJ cell.

### A. Use of all base-collector tunnel barriers to ensure current-voltage asymmetry

In this first section, we focus on the current asymmetry which can be induced using the base-collector tunnel barrier. In order to evaluate the device, we use the current asymmetry defined as the ratio  $J_C(|V_{CB}|)/J_C(-|V_{CB}|)$ , which varies with  $V_{CB}$ . A constant bias voltage is applied to the emitter-base junction which injects a current of hot electrons in the base. The current of hot electrons is allowed to be injected in the collector electrode depending on the bias voltage of the base-collector junction as depicted in Fig. 1(a). The  $V_{CB}$  voltage controls the asymmetry of the device and, when negatively biased, stops the current of hot electrons. The computations have been done using parameter values close to those evaluated experimentally:  $d_1$  and  $d_2$  have been taken equal to 1 and 4 nm while  $\phi_1$  and  $\phi_2$  values are 1.5 and 0.5 eV, respectively. In the following, characteristic (collector current)/(base-collector voltage), (collector current asymmetries)/(base-collector voltage) and (collector current magneto resistance)/(base-collector voltage) are shown for different emitter-base voltages.

It appears that the asymmetry in the collector current depends strongly on the emitter-base bias voltage and so on the energy of the hot electrons [Fig. 2(a)]. As expected, the higher asymmetries are observed when the emitter-base voltage is close and a bit higher than the barrier height of the base-collector junction,  $\phi_2$ . Then, asymmetries above 10 000 in the forward and backward collector currents can be observed [Fig. 2(b)]. As a matter of fact, the base-collector voltage range in which the current asymmetry is above a given value depends on the emitter-base voltage (Table I). Current asymmetries above 1000 are easily reached for a large range of base-collector voltages. For specific applications, if lower asymmetries are needed, they can be obtained in a larger voltage range. For example, with  $V_{BE}=0.6$  V, an asymmetry above 25 is expected for a  $V_{CB}$  range of 0.44 V. This voltage range decreases to 0.17 V (Table I) when an asymmetry above 1000 is needed. Furthermore, the level of TMR in the collector current remains high and quite constant, especially for the most interesting 0.6 V bias voltage, as shown in Fig. 2(c). One major advantage of this use is the fact that applied voltages are far away from the known breakdown voltages of such tunnel barriers. In conclusion, considering the transport of hot electrons without coherence in a 3TD-MTJ in which only the base-collector junction ensures the asymmetry, it is reasonable to observe large spin-polarized collector current asymmetries.

### B. Use of all 3TD-MTJ's to ensure current-voltage asymmetry

In this second section, we focus on the current asymmetry which can be induced using all the structure. In this application, we consider a zero constant bias voltage applied to the

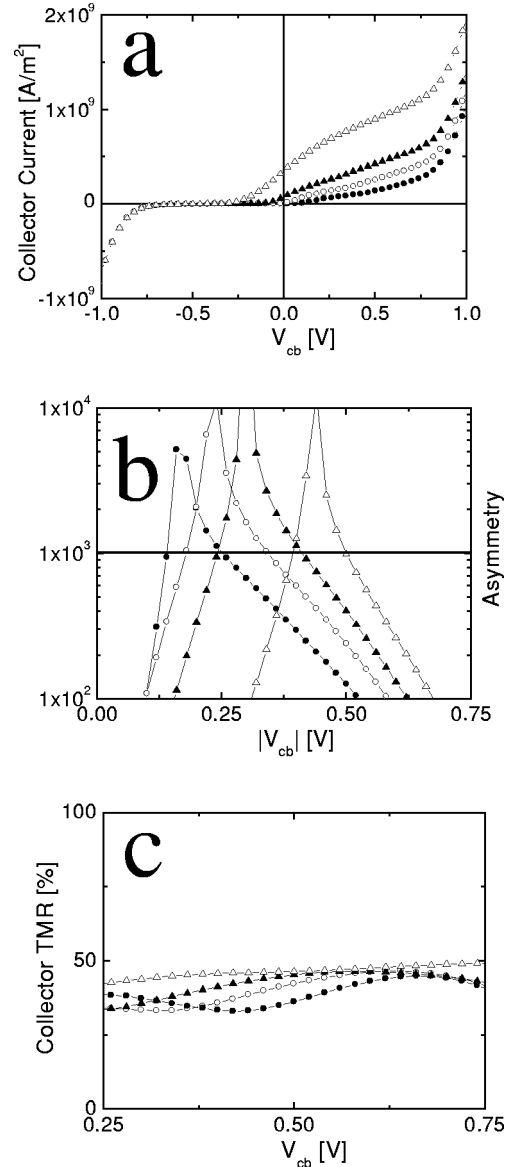


FIG. 2. Characteristics of the device as a function of the base-collector voltage  $V_{CB}$  at various fixed emitter-base voltage  $V_{BE}$  of 0.5 V (disk), 0.55 V (open disk), 0.6 V (triangle), and 0.7 V (hollow triangle). (a) Collector current, (b) asymmetry of the collector current, and (c) magnetoresistance of the collector current (normalized by the collector current in the antiparallel configuration which corresponds to the magnetization of the base antiparallel to those of the emitter and the collector).

base-collector junction and use all the structure to ensure the current asymmetry. When the emitter-base junction is polarized positively at bias voltages above  $\phi_2$ , a current of hot electrons is allowed to be injected in the collector electrode. Inversely, when the emitter-base junction is polarized negatively, no current is extracted from the collector electrode. Therefore, an infinite collector current asymmetry is expected from this way of the hot-electron three-terminal device use [Fig. 3(a)]. The computations have been done using the same parameter values as for the last paragraph. We have varied the thickness of the base and also the thickness of the base-collector tunnel barrier.

TABLE I. Minimum and maximum  $V_{BC}$  voltages for which an asymmetry in collector current above 1000 have been calculated as a function of  $V_{EB}$  voltage. The last column shows the  $V_{BC}$  voltage window.

$V_{BE}$ [V]	$V_{CBmin}$ [V]	$V_{CBmax}$ [V]	$\Delta V_{CB}$ [V]
0.5	0.14	0.254	0.114
0.55	0.18	0.343	0.163
0.6	0.243	0.414	0.171
0.7	0.39	0.5	0.11

First of all, no effect of the base-collector barrier thickness could be observed, except for the TMR signal. Indeed, when the emitter-base junction is negatively polarized, the collector current is zero independently of the barrier thickness. When polarized positively, the electrons injected from the emitter-base junction seem not to be so sensitive to the thickness of the second tunnel barrier. Then, we have fixed the thickness of the insulating barrier layer of the base-collector junction to 2 nm and we have changed the thickness of the base. Since the current asymmetry is infinite, the choice of the resistance of the 3TD-MTJ and the value of TMR desired for the specific application of the asymmetric diode is driven by the base thickness. As shown in Fig. 3(b), the increase of the base thickness will increase the resistance of the 3TD-MTJ but also the value of TMR. This can be

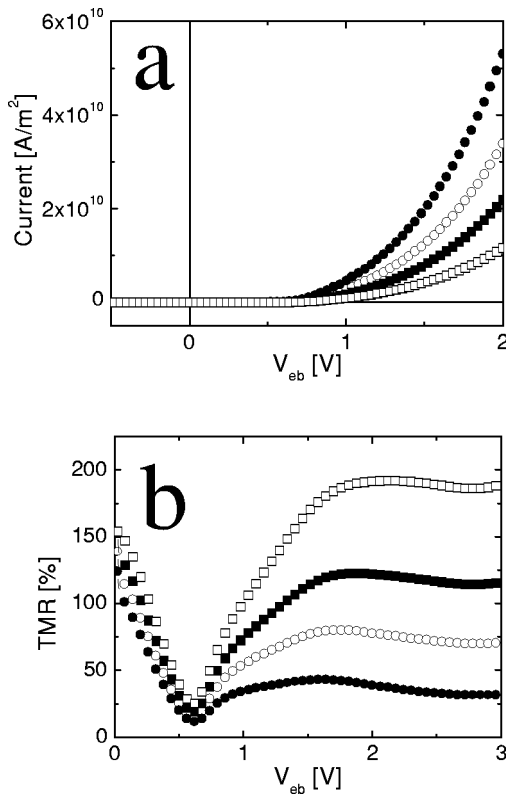


FIG. 3. (Collector current)/(emitter-base voltage) (a) and (collector TMR)/(emitter-base voltage) (b) characteristics computed as a function of base thickness: 3 nm (disk), 5 nm (hollow disk), 7 nm (square), and 10 nm (open square).

understood considering that, first of all, the thickness of the base, via the mean free path of the hot electrons, controls the collector current and so the resistance of the device. Furthermore, the mean free path is spin dependent and so increasing the base thickness will increase the contrast between the spin-up and spin-down hot-electron current (as in the hot electron spin-valve transistor<sup>13</sup>). Therefore, a highly polarized hot-electron current is injected into the  $I_2/M_3$  collector and an increase of TMR is observed. This last result is at the origin of the new concept of an *artificial half metal* composed by the  $M_1/I_1/M_2$  injection structure which is able to provide a highly polarized hot-electron current.

A similar concept of diodes has been proposed<sup>29</sup> and realized experimentally recently<sup>30</sup> without an electric contact taken at the base electrode. A current asymmetry of 25 was observed, resulting from coherent hot-electron transport in an  $M_1/I_1/M_2/I_2/M_3$  structure in which (i)  $\phi_{I1} \approx 2\phi_{I2}$  and (ii)  $d_{I1} \approx 2d_{I2}$ . In this case, the current asymmetry was ensured by the main voltage drop on the first  $I_1$  barrier. So, positively biased, the electrons injected from  $M_1$  to  $M_2$  have enough energy to overcome  $I_2$  and reach  $M_3$ . Inversely, when negatively biased, the electrons have to overcome both  $I_1$  and  $I_2$ . A substantial improvement of the diode characteristics is achieved by control of the base voltage as shown in this section. Indeed, this control ensures a larger current asymmetry without the need for resonance to enhance the coherent-transport-induced asymmetry<sup>29</sup>. Furthermore, it softens the window of barrier parameters [(i) and (ii)] required to have the proper drop of emitter-base voltage and so allows the use of many  $I_1$  and  $I_2$  couples.

#### IV. TRANSISTOR APPLICATION

As depicted in Ref. 11, the 3TD-MTJ can be used as a transistor and this in several voltage windows. But as will be shown in the following, the use of magnetic electrodes adds a new functionality since it allows control and a nonvolatile programming of the current-voltage characteristics of the device.

First of all, as presented in the previous section, operating the 3TD-MTJ with  $V_{CB}$  near the crossover voltage for which  $J_C = 0$  leads to an appreciable transconductance  $J_C/V_{CB}$ . Indeed, due to the strong variation of tunneling with a small variation of barrier height, the transmission of the hot electrons is expected to vary significantly with  $V_{CB}$ . Furthermore, this transconductance increases with injection energy  $V_{BE}$ .

Nevertheless, we would like to concentrate this section on the operation window first exemplified in Ref. 11. A constant bias voltage is applied to the emitter-base junction which injects a current of hot electrons in the base. When the base-collector junction is positively biased, much of those electrons are transmitted to the collector while a small part is thermalized in the base. The ratio depends on the applied voltages and the parameters of the base (mean free path, thickness). This transistor acts as a conventional bipolar transistor but the electrons in the base are not thermalized and combining electron and holes in the base to make the base

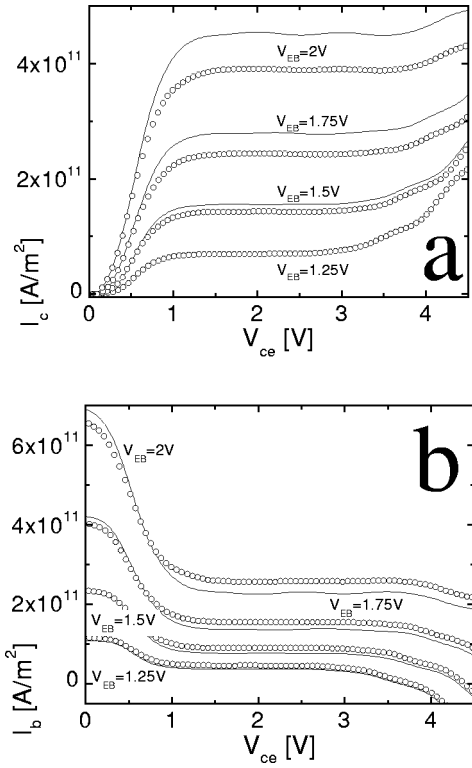


FIG. 4. (Collector current)/(emitter-collector voltage) (a) and (base current)/(emitter-collector voltage) (b) characteristics computed as a function of emitter-base voltage and magnetic configuration for a 3TD-MTJ structure with two 0.5-eV-height barriers and barrier thickness  $d_1$  and  $d_2$  equal to 2 and 5 nm.

current is replaced by elastic and inelastic scattering. Nevertheless, common emitter characteristics look the same. They have been computed using a 3TD-MTJ structure with two 0.5-eV-height barriers with thicknesses  $d_1$  and  $d_2$  equal to 2 and 5 nm. From our experience and published results,<sup>31</sup> conventional  $\text{Al}_2\text{O}_3$  barriers have breakdown voltages around 2 V or less. But the operating voltage of the injection junction is around this value. Then, we have chosen the parameters of TaO for both barriers since the breakdown voltage of those barriers appeared much higher.<sup>26</sup> Nevertheless, calculations (not shown) have also been done with the  $\text{Al}_2\text{O}_3$  barrier parameters and similar effects have been obtained.

In Fig. 4, magnetic-configuration-dependent  $J_B(V_{CE})$  and  $J_C(V_{CE})$  characteristics are shown as a function of  $V_{BE}$ , the emitter-base voltage. The current gain is defined by  $\beta = J_C(V_{CE})/J_B(V_{CE})$ . Even if the current gain  $\beta$  is low for the set of junction parameters used (around two for those calculations), a clear transistor effect is observed and  $\beta$  varies with the orientation of the magnetization of  $M_2$ .

From the physical point of view, the appearance of a large plateau in the  $J_B(V_{CE})$  and  $J_C(V_{CE})$  characteristics for  $V_{CE}$  between 1 and 3 V is linked to the saturation of the hot-electron current. Then, when  $V_{CE}$  is increased above 3 to 4 eV (depending on  $V_{BE}$ ), the additional increase of collector current originates from the tunneling of “cold” electrons injected from the base into the collector and not more from the emitter to the collector (this current is saturated). So we have the appearance of nonlinearity originating from the signature

of electron tunneling from “cold” electrons injected from the base into the collector. A larger plateau can then be reached by increasing the base-collector junction resistance and thus the thickness  $d_2$ ; here,  $\phi_2$  can also be increased but a higher  $V_{BE}$  is then needed to get a proper working of the device. The voltage offset in  $V_{CE}$  observed before the  $J_C$  plateau is controlled by  $\phi_1$ . Indeed, calculations using  $\phi_1 = 1.5$  eV have shown that the inflection of the  $J_C(V_{CE})$  curve is shifted from 0.6 eV [Fig. 4(a)] to around 1.4 eV.

From our point of view, the main challenge is to increase the current gain  $\beta$ . Calculations have been done with a reduced base thickness and/or a larger  $\lambda$ ; it follows that a larger spin-dependent current gain can be reached. Indeed, in both cases, considering  $V_{BE}$  and  $V_{CB}$  fixed, a strong reduction of the base current is expected in our model and this is mainly linked to the exponential dependence with base thickness of the probability of an electron to be thermalized. Since  $\beta$  is the ratio of the collector current and the base current, a strong increase of  $\beta$  can be observed.

It has been shown that an electric contact can be taken on a base layer as thin as 1.9 nm,<sup>11</sup> but this constitutes a real technological bottleneck. Nevertheless, we can be optimistic about this point.<sup>14</sup> Work can also be done on the material used to grow the base. Indeed, the important parameter is the mean free path of the hot electrons,  $\lambda$ . Only few data are actually available in the energy range of interest here. Nevertheless at those energies, the main source of electron scattering is plasmons,<sup>9</sup> and reducing or increasing their energy with respect to the hot-electron injection energy will increase  $\lambda$ . For example, the plasmon energy can be reduced by tailoring the band structure of the base to decrease its density of states at the Fermi level. This has been done in Ref. 11 with the use of a  $\text{CoSi}_2$  base, for which the experimental data could be reproduced with our model by introducing  $\lambda = 100$  nm. This value is in agreement with the one extracted by the authors [ $\lambda > 50$  nm (Ref. 32)]. Then, even if the base is not magnetic, a spin-dependent transport could be observed if the base thickness is thinner than its spin diffusion length. However, our model does not support the use of  $\lambda$  values much larger than the thickness of the base (2 nm in Ref. 11). In this case, indeed, coherent transport through the base has to be considered while a complete phase relaxation was used in our model. Nevertheless, this result shows that the computed currents are underestimated in comparison to those measured in real systems. Since our model underestimates the current, it is not surprising that we have to enter a larger mean free path in the calculations to reproduce the experimental data.

## V. CONCLUSIONS

A large part of this paper has been devoted to possible future applications of 3TD-MTJ structures. But besides for their applied interest,  $M_1/I/M_2/I/M_3$  structure can be used to measure the properties of nonequilibrium spin-dependent hot-electron transport in the range of 0.5–4 eV. This energy range is difficult to access with non-solid-integrated electron injection sources. Some experimental results have been reported recently with integrated spin-valve transistors.<sup>19,27,33</sup>

The different contributions to the hot-electron mean free path can be discriminated and those results supply theoretical developments with data. On the other hand, the properties of insulating materials used for the base-collector junction can also be studied. Indeed, injecting hot electrons into a barrier allows us to study its electric transport processes without applying high to voltages to its electrodes. So the existence of a Poole-Frenkel transport mechanism can be checked even for low-breakdown-voltage junctions.

The concept of 3TD-MTJ structures with high asymmetry of backward to forward currents or with transistorlike characteristics has been theoretically demonstrated. In these cal-

culations, the set of junction parameters was chosen to fit experimental conditions that can be reached in the near future in order to bring soon an experimental verification of those calculations. Work is under progress.

#### ACKNOWLEDGMENTS

The authors thank P. Rottländer, C. Tiusan, and J. Gregg for valuable discussions. This work is supported by the EC-IST program "NanoMEM," No. IST-1999-13471. This work is partially supported by "La Région Lorraine."

- <sup>1</sup>J.S. Moodera, L.R. Kinder, T.M. Wong, and R. Meservey, *Phys. Rev. Lett.* **74**, 3273 (1995).
- <sup>2</sup>S.A. Wolf, *J. Supercond.* **13**, 195 (2000).
- <sup>3</sup>C.H. Shang, J. Nowak, R. Jansen, and J.S. Moodera, *Phys. Rev. B* **58**, R2917 (1998); R. Jansen and J.S. Moodera, *J. Appl. Phys.* **83**, 6682 (1998); R.C. Sousa, J.J. Sun, V. Soares, P.P. Freitas, A. Kling, M.F. da Silva, and J.C. Soares, *Appl. Phys. Lett.* **73**, 3288 (1998).
- <sup>4</sup>M. Hehn, O. Lenoble, D. Lacour, C. Féry, M. Piécuch, C. Tiusan, and K. Ounadjela, *Phys. Rev. B* **61**, 11 643 (2000).
- <sup>5</sup>R.E. Dunin-Borkowski, M.R. McCartney, D.J. Smith, S. Gider, B.U. Runge, and S.S. Parkin, *J. Appl. Phys.* **85**, 4815 (1999); C. Tiusan, T. Dimopoulos, M. Hehn, V. Da Costa, Y. Henry, H.A.M. van den Berg, and K. Ounadjela, *Phys. Rev. B* **61**, 580 (2000).
- <sup>6</sup>M. Jullière, *Phys. Lett.* **54A**, 225 (1975); J.C. Slonczewski, *Phys. Rev. B* **39**, 6995 (1989); I.I. Mazin, *Phys. Rev. Lett.* **83**, 1427 (1999).
- <sup>7</sup>F. Montaigne, M. Hehn, and A. Schuhl, *Phys. Rev. B* **64**, 144402 (2001).
- <sup>8</sup>I.I. Oleinik, E.Y. Tsymlal, and D.G. Pettifor, *Phys. Rev. B* **62**, 3952 (2000); J.M. MacLaren, X.G. Zhang, W.H. Butler, and X. Wang, *ibid.* **59**, 5470 (1999).
- <sup>9</sup>C.A. Mead, *J. Appl. Phys.* **32**, 646 (1961).
- <sup>10</sup>F. Montaigne, J. Nassar, A. Vaures, F. Nguyen Van Dau, F. Petroff, A. Schuhl, and A. Fert, *Appl. Phys. Lett.* **73**, 2829 (1998).
- <sup>11</sup>S. Muratake, M. Watanabe, T. Suemasu, and M. Asada, *Electron. Lett.* **28**, 1002 (1992); W. Saitoh, T. Suemasu, Y. Kohno, M. Watanabe, and M. Asada, *Jpn. J. Appl. Phys., Part 2* **34**, L1254 (1995).
- <sup>12</sup>M. Heiblum, D.C. Thomas, C.M. Knoedler, and M.I. Nathan, *Appl. Phys. Lett.* **10**, 1105 (1985).
- <sup>13</sup>D.J. Monsma, R. Vlutters, and J.C. Lodder, *Science* **281**, 407 (1998).
- <sup>14</sup>S. Stein, R. Schmitz, and H. Kohlstedt, *Solid State Commun.* **117**, 599 (2001).
- <sup>15</sup>A. Filipe, H.-J. Drouhin, G. Lampel, Y. Lassailly, J. Nagle, J. Peretti, V.I. Safarov, and A. Schuhl, *Phys. Rev. Lett.* **80**, 2425 (1998).
- <sup>16</sup>D. Oberli, R. Burgermeister, S. Riesen, W. Weber, and H.C. Siegmann, *Phys. Rev. Lett.* **81**, 4228 (1998).
- <sup>17</sup>J. Hong and D.L. Mills, *Phys. Rev. B* **59**, 13840 (1999).
- <sup>18</sup>W.H. Rippard and R.A. Buhrman, *Phys. Rev. Lett.* **84**, 971 (2000).
- <sup>19</sup>R. Vlutters, O.M.J. van 't Erve, S.D. Kim, R. Jansen, and J.C. Lodder, *Phys. Rev. Lett.* **88**, 027202 (2002).
- <sup>20</sup>S. Zhang, *J. Appl. Phys.* **87**, 5218 (2000).
- <sup>21</sup>A. Filipe, Ph.D. thesis, Ecole Polytechnique, 1997.
- <sup>22</sup>R. Tsu and L. Esaki, *Appl. Phys. Lett.* **22**, 562 (1973).
- <sup>23</sup>S. Zhang, P.M. Levy, A.C. Marley, and S.S.P. Parkin, *Phys. Rev. Lett.* **79**, 3744 (1997).
- <sup>24</sup>J.M. De Teresa, A. Barthélémy, A. Fert, J.P. Contour, R. Lyonnet, F. Montaigne, P. Seneor, and A. Vaures, *Phys. Rev. Lett.* **82**, 4288 (1999).
- <sup>25</sup>A.H. Davis and J.M. MacLaren, *J. Appl. Phys.* **87**, 5224 (2000).
- <sup>26</sup>P. Rottländer, M. Hehn, O. Lenoble, and A. Schuhl, *Appl. Phys. Lett.* **78**, 3274 (2001).
- <sup>27</sup>R. Vlutters, R. Jansen, O.M.J. van 't Erve, S.D. Kim, and J.C. Lodder, *J. Appl. Phys.* **89**, 7305 (2001).
- <sup>28</sup>W. J. Gallagher, J. H. Kaufman, S. S. P. Parkin, and R. E. Scheuerlein, United States Patent No. 5,640,343, June 17, 1997.
- <sup>29</sup>M. Chshiev, D. Stoeffler, A. Vedyayev, and K. Ounadjela, *Europhys. Lett.* **58**, 257 (2002).
- <sup>30</sup>C. Tiusan, M. Chshiev, A. Iovan, V. da Costa, D. Stoeffler, T. Dimopoulos, and K. Ounadjela, *Appl. Phys. Lett.* **79**, 4231 (2001).
- <sup>31</sup>W. Oepts, H.J. Verhagen, W.J.M. de Jonge, and R. Coehoorn, *Appl. Phys. Lett.* **73**, 2363 (1998).
- <sup>32</sup>The transfer efficiency of hot electrons with monochromatic energy across a 1.9-nm-thick metal (CoSi<sub>2</sub>) epitaxial layer was estimated to be more than 0.96 from negative differential resistance characteristics of a metal(CoSi<sub>2</sub>)/insulator(CaF<sub>2</sub>) quantum interference transistor. Such a high value of transfer efficiency may be due to the very thin single-crystalline metallic layer. From this transfer efficiency, mean free path of hot electrons is estimated to be more than 50 nm. WEB site <http://www.pe.titech.ac.jp/Suemasu/ResearchReview/95/act295.htm>. T. Suemasu, Y. Kohno, W. Saitoh, M. Watanabe, and M. Asada, *IEEE Trans. Electron Devices* **42**, 2203 (1995).
- <sup>33</sup>R. Jansen, S.D. Kim, R. Vlutters, O.M.J. van 't Erve, and J.C. Lodder, *Phys. Rev. Lett.* **87**, 166601 (2001).